

Optimization of ethyl oleate from oleic acid and ethanol with Dean-Stark trap technology by response surface methodology

Sri Budi Harmami^{1,2}, Yenny Meliana², Puji Wahyuningsih³, and Misri Gozan^{1,4*}

¹Department of Chemical Engineering, Faculty of Engineering, Universitas Indonesia, Kampus UI Depok, 16424, Indonesia

²Research Center for Chemistry, National Research and Innovation Agency (BRIN), PUSPIPTEK Area, Serpong, Tangerang Selatan, Banten, 15314, Indonesia

³Department of Informatics Engineering, Faculty of Engineering, Universitas Muhadi Setiabudi, Brebes, 52212, Indonesia

⁴Research Centre for Biomass Valorization – Universitas Indonesia (RCBV UI), Faculty of Engineering, Universitas Indonesia, Kampus UI Depok, 16424, Indonesia

Abstract. This work evaluates the optimum condition of the esterification reaction of oleic acid (OA) and ethanol by Dean-Stark trap (DS) and without technology, as well as the effects of the various factors' interaction on the conversion rate of OA. The influences of OA/ethanol molar ratio, concentration of catalyst, temperature reaction, and time reaction on the conversion rate of OA were investigated. The response surface method (RSM) is combined to optimize the experimental scheme. The results showed that the conversion rate of OA reached the peak of 98.78% when the molar ratio of ethanol/OA was 9:1, the concentration of catalyst was 3%, the temperature reaction was 90 °C, and the reaction time was 10 hours. Compared with the esterification reaction without DS, the conversion rate of OA was 54.96%. FTIR analysis confirmed the changes of a functional group for the response, and GC-MS was for confirmation of the fragmentation mode of the esterification reaction that occurs. The availability of ethyl oleate derived from palm oil, aimed at surfactant production, provides an excellent feedstock to produce surfactants for cosmetic applications.

1 Introduction

Esterification is one of the most significant reactions in the organic synthesis process. Esterification reactions are commonly used in various industrial processes and laboratory syntheses to produce esters, which have a wide range of applications[1]. Many industrial sectors, especially cosmetics for applications, include the production of perfume additives[2]; [3]flavors, fragrances[4], surfactants, and personal care product formulations[5][6][7] as many naturally occurring compounds are esters. A typical Fisher esterification reaction involves heating between a carboxylic acid and an excess amount of the corresponding alcohol in the presence of a catalyst, like an esterification reaction between oleic acid and ethanol with sulfuric acid as a catalyst, which is shown in Figure 1. Jyoti et al. conducted an

Corresponding author: ^{1,3}mgozan@ui.ac.id (M. Gozan)

experiment on the esterification of acrylic acid with ethanol using catalyst variations such as hydrochloric acid, hydroiodic acid, and sulfuric acid. The conversion of acrylic acid was 83.99 % at 70C, the catalyst concentration was 3 %, and the ethanol/acrylic acid molar ratio was 1:1[8]. A Dean-Stark trap (DS) method was used to collect water as a byproduct of the esterification reaction. It can drive the equilibrium in reactions to move the right side. The esterification reaction is reversible, where water is formed as a byproduct [9].

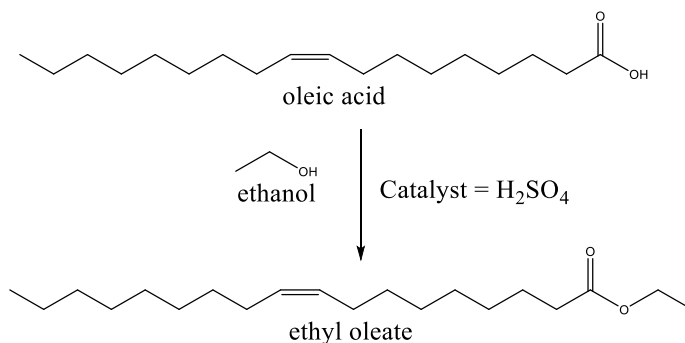


Fig 1. Transformation of oleic acid into ethyl oleate using H₂SO₄ as the catalyst

Response surface methodology (RSM) is a combination of statistical and mathematical techniques for empirical model building[10]. RSM is used for modeling and analyzing the desired response when several variables influence the response, and the goal is to optimize these responses[11]. The research was conducted to optimize biodiesel production from cow tallow using RSM with the software Design Expert 7.0.0[12]. The transesterification reaction uses sodium hydroxide as a catalyst and methanol as a solvent. Naidir et al., conducted research optimization of epoxidized trimethylolpropane ester from palm oil using RSM. The response of a percentage of oxirane oxygen value, iodine value, and hydroxyl value with free variables, namely reaction time, temperature reaction, and glacial acetic acid concentration[13]. Manga et al. do research on the optimization synthesis of fatty acid ethyl ester as biodiesel from palm fatty acid using SO₄²⁻/TiO₂ catalyst[14].

This research focuses optimization on the effect of temperature reaction, catalyst concentration, ethanol/OA molar ratio, and reaction time on the OA conversion from esterification reaction with oleic acid and ethanol. As well as knowing the identification of components and molecular structure of ethyl oleate with/without a Dean-Stark trap technology.

2 Materials and Methods

2.1 Materials

Oleic acid from PT. Sanbio Laboratories, Indonesia (acid value 208 mg KOH/g), sulfuric acid (98%), potassium hydroxide (pro analysis), and ethanol (absolute for analysis) were purchased from Merck, Germany. The phenolphthalein as an indicator when calculating acid value was purchased from Sigma Aldrich.

2.2 Methods

2.2.1 Esterification-Dean Stark trap reaction

As shown in Fig. 1, the reactant prepared according to a certain molar ratio of OA and ethanol are added to a three-necked flask for heating with various temperature (80 °C, 90 °C, and 100 °C), with various reaction time (8, 10, 12 hours), various ethanol/OA molar ratio (9:1; 10:1; and 12:1), various catalyst concentration (1 %, 2 %, and 3 %), and the magnetic stirring speed was 500 rpm. A reflux condenser was placed above the three-necked flask to reduce the evaporation loss of the reactants. The added catalyst (H₂SO₄) with drop by drop. The process was conducted with a dean-stark trap (DS) and without a dean-stark trap (DSO). Furthermore, the ethyl oleate was carried out to characterize the molecular structure with Fourier Transform Infra-Red (FTIR), Gas chromatography-mass spectrometry (GC-MS), and calculated acid value. The acid value of the sample is determined by titration, and the conversion rate of OA is figured up by measuring the acid value and performing an arithmetic average to reduce errors, shown as the following formula (1):

$$\text{Acid value} = \frac{V_{\text{KOH}} \times C_{\text{KOH}} \times 56.1}{m_0} \quad (1)$$

Where V_{KOH} represents the volume of KOH standard solution consumed by titration (ml), C_{KOH} refers to the standard solution concentration of KOH (mol/ml), 56.1 is the relative molar mass of KOH (g/mol), and m_0 represents the mass of the titrated sample (g). After the acid value of the sample is determined by the titration method, the conversion rate of OA is calculated by the following formula (2):

$$\text{OA conversion rate} = \frac{A_a - A_b}{A_a} \times 100\% \quad (2)$$

In this formula, A_a represents the acid value (mg/g) of OA before the reaction, and A_b is the product's acid value (mg/g) after the reaction.

2.2.2 The characterization of the molecular structure with FTIR

Characteristic molecular structures like functional groups of esterification reaction samples were examined by a Tensor II FTIR Spectrometer (Bruker, Co., Ltd., Germany) with a standard KBr beamsplitter. The spectra rate is 25 spectra per second with the scope of 500-4000 cm⁻¹ and measurement at 25 ± 1 °C.

2.2.3. Gas chromatography-mass spectrometry (GC-MS) analysis

GC-MS spectra were carried out in an Agilent 7890B (GC) and 5977A as mass spectra detector (MSD) using column type (HP-5 phase 30 m x 0.32 mm x 0.25 μm), with the injector set at 250 °C. The detector temperature was 300 °C, using H₂ as the carrier gas at a 30 mL/min flow rate, airflow was 400 mL/min, and makeup flow (N₂) was 25 mL/min. The injection mode uses 7693A with an injection volume of 1 μL. The data was analyzed over a mass per charge (m/z) range of 145-905 and identified by comparing the mass spectra with the NIST (National Institute of Standards and Technology) mass spectral library. NIST uses the

submitted unknown spectrum collected by mass spectrometer detectors (MSD) and performs a library spectrum search. NIST MS search 2.3 was used for mass spectra comparison[15].

2.2.4 Experimental design and optimization based on RSM

In the esterification reaction, the single-factor experiment method is applied to explore the influence of each impacting factor on the esterification conversion rate. However, this always ignores the result of the interaction between variables [16]. In this research, in order to optimize the impact of each variable's synergistic effect on the OA conversion rate, a combination of RSM and Box-Behnken Design (BBD) was used to optimize the experimental scheme[17] [16]. The conversion of OA (Y) was chosen as the response variable. In contrast, the temperature reaction (X_1), concentration of catalyst (X_2), molar ratio of ethanol/OA (X_3), and reaction time (X_4) were chosen as free variables. These variables were potential critical parameters with range levels (low and high) that would set a two-level observation for each free variable summarized in Table 1. The Design-Expert v13 software (trial version, Stat-Ease Inc., Minneapolis, USA) was used to fit the experimental data into the quadratic polynomial regression equation of the following formula (3), and the influence of the interaction between various factors on the OA conversion rate could be observed, through the obtained 3D response surface graph.

$$Y = \beta_0 + \sum_{i=1}^n \beta_i x_i + \sum_{i=1}^n \beta_{ii} x_i^2 + \sum_{i=1}^{n-1} \sum_{i < j=2}^n \beta_{ij} x_i x_j \quad (3)$$

Where Y is the response value, β_0 is the regression equation constant, β_i refers to the linear coefficient, β_{ii} is the quadratic coefficient, β_{ij} represents the interaction coefficient, n is the number of the independent variable, and x_i and x_j separately are the independent variables.

In the analysis of variance (ANOVA)[18] the F value represents the fit of the corresponding factor, and a larger F value would lead to a more significant corresponding factor. The p-value indicates the significance level of the model and parameters. The P value of <0.050 illustrates that the model is significant at >95 % confidence intervals. Finally, the optimal reaction conditions for maximizing the OA conversion rate are obtained through the model optimization experimental plan.

Table 1. Experimental range levels of esterification reaction variables in BBD

Variables	Coded value	Range level	
		Low	High
Temperature reaction (°C)	X_1	80	100
Catalyst concentration (%)	X_2	1	3
Ethanol/OA molar ratio (mol)	X_3	9	12
Reaction time (hour)	X_4	8	12

3 Results and Discussion

3.1 Esterification profile analysis by GC-MS

The compound identification of esterification reaction using GC-MS to analyze the esterification reaction of oleic acid and ethanol with or without a Dean-stack trap, defining

their retention times and MS breakage fragments. The chromatograms and compositions of the samples are reported in Fig. 2, 3, 4, and Table 2, respectively.

Table 2. List of compounds present in the oleic acid and esterification profile with GC-MS analysis

Retention time (min)	Peak Area (%)	Assigned formula	Assigned compound	Molecular ion mass (g/mol)	Equal to
<i>Oleic acid sample</i>					
23.600	5.60	C ₁₆ H ₃₂ O ₂	Palmitic acid (n-hexadecanoic acid)	256.42	86
25.146	36.43	C ₁₈ H ₃₂ O ₂	Linoleic acid (9,12-octadecadienoic acid)	280.44	94
25.196	52.63	C ₁₈ H ₃₄ O ₂	Oleic acid (9-octadecenoic acid)	282.46	80
25.380	5.16	C ₁₈ H ₃₆ O ₂	Stearic acid (octadecanoic acid)	284.47	93
27.015	0.18	C ₂₀ H ₃₂ O ₂	Arachidic acid, TMS derivative	304.46	81
<i>Esterification reaction with the DS method</i>					
23.086	4.36	C ₁₇ H ₃₄ O ₂	Heptadecanoic acid, methyl ester	270.45	91
23.600	0.74	C ₁₆ H ₃₂ O ₂	Palmitic acid (n-hexadecanoic acid)	256.42	86
24.733	67.13	C ₂₀ H ₃₈ O ₂	Ethyl oleate ((E)-9-octadecenoic acid ethyl ester)	310.51	83
24.933	4.73	C ₂₀ H ₄₀ O ₂	Ethyl stearate (Octadecanoic acid, ethyl ester)	312.53	94
25.155	0.85	C ₁₈ H ₃₄ O ₂	Oleic acid (9-octadecenoic acid)	282.46	86
26.250	2.66	C ₂₀ H ₄₀ O ₂	Ethyl stearate	312.53	59
26.365	1.03	C ₂₀ H ₄₀ O ₂	Ethyl stearate	312.53	78
26.431	2.32	C ₂₀ H ₄₀ O ₂	Ethyl stearate	312.53	44
26.625	1.65	C ₂₀ H ₄₀ O ₂	Ethyl stearate (eicosanoic acid, ethyl ester)	312.53	83
26.860	3.33	C ₁₈ H ₃₆ O ₂	Ethyl palmitate (ethyl hexadecanoate)	284.47	18
28.100	0.76	C ₅ H ₁₀ O	Pentanoic acid (2-phenylethyl ester)	102.13	35
<i>Esterification reaction without the DS method</i>					
23.087	2.64	C ₁₆ H ₃₂ O ₂	Palmitic acid (Hexadecanoic acid, ethyl ester)	256.42	91
23.600	1.00	C ₁₆ H ₃₂ O ₂	Palmitic acid, TMS derivative	256.42	80
24.715	36.03	C ₂₀ H ₃₈ O ₂	Ethyl oleate ((E)-9-octadecenoic acid ethyl ester)	310.51	83

24.933	2.89	C ₂₀ H ₄₀ O ₂	Ethyl stearate (octadecanoic acid, ethyl ester)	312.53	94
25.161	1.07	C ₁₈ H ₃₄ O ₂	Oleic acid (9-octadecenoic acid)	282.46	87
25.417	16.15	C ₂₉ H ₅₀ O	Gamma-sitosterol	414.70	99
26.251	14.96	C ₆ H ₈ O ₂	Cyclopentene-4-carboxylic acid, methyl ester	112.12	27
26.391	14.35	C ₂₀ H ₄₀ O ₂	Ethyl stearate	312.53	72
26.627	0.76	C ₂₀ H ₄₀ O ₂	Ethyl stearate (eicosanoic acid, ethyl ester)	312.53	91
26.862	0.55	C ₁₈ H ₃₆ O ₂	Ethyl palmitate (ethyl hexadecanoate)	284.47	22
27.764	2.74	C ₂₀ H ₄₀ O ₂	Ethyl stearate	312.53	59
28.210	0.65	C ₅ H ₁₀ O	Pentanoic acid (2-phenylethyl ester)	102.13	49

Analysis of MS spectra comparison using a mass spectral library search with release version 2023.09 corroborated the formation of ethyl oleate. Figure 2 represents the resulting GC-MS of oleic acid as a main reactant. The assigned compound, retention time, peak area, assigned formula, molecular ion mass, and qual are displayed in Table 2. The major dominant component in terms of (% peak area) in oleic acid profile was there were five compounds in the fraction were identified as oleic acid (C₁₈H₃₄O₂, 52.63 %), palmitic acid (C₁₆H₃₂O₂, 5.6 %), linoleic acid (C₁₈H₃₂O₂, 36.43 %), stearic acid (C₁₈H₃₆O₂, 5.16 %), and arachidic acid TMS derivatives (C₂₀H₃₂O₂, 0.18 %). The resulting esterification reaction with the DS method is shown in Fig. 3 and Table 2. One of the main compounds in the fraction with a peak area of 67.13 % was identified as ethyl oleate (C₂₀H₃₈O₂), with a qual score of 80 correspondence for 9-octadecenoic acid. The qual is the measured value of the direct match of peak m/z values and relative intensities. NIST uses a scale of 0-100 if a scale of >90 is an excellent match, a scale of 80-900 is a good match, a scale of 70-80 is a fair match, and a scale of <60 is a poor match (NIST mass spectral library). At the same time, the esterification reaction without the DS method (Fig. 4 and Table 2) generated ethyl oleate with a peak area of 36.03 for a qual score of 83.

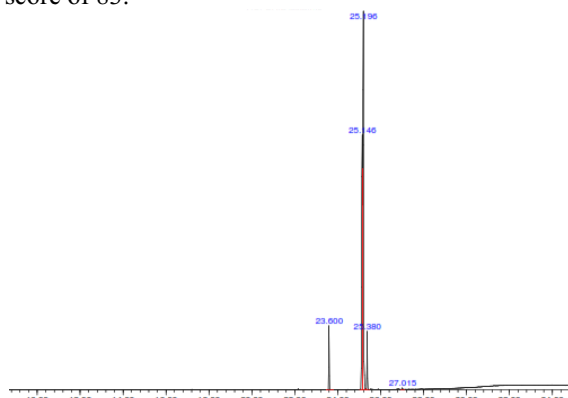


Fig. 2. Chromatograms obtained by monitoring the total ion current (TIC, scan mode) in the GC-MS system of oleic acid

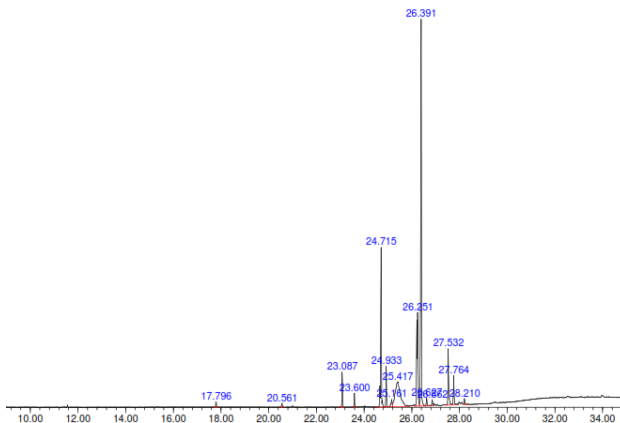


Fig. 3. Chromatograms obtained by monitoring the total ion current (TIC, scan mode) in the GC-MS system of the esterification ethanol and OA with DS method

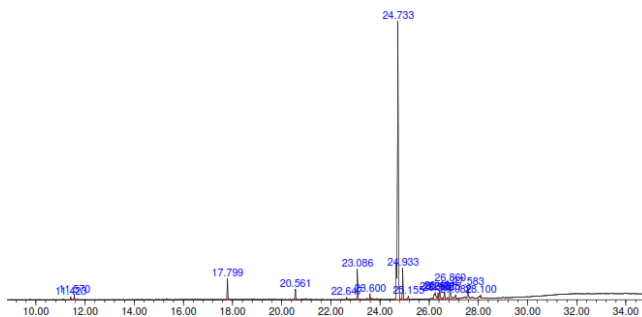


Fig. 4. Chromatograms obtained by monitoring the total ion current (TIC, scan mode) in the GC-MS system of the esterification ethanol and OA without DS method

3.2 Molecular structure by FTIR

The molecular structure, especially functional groups of the esterification reaction between oleic acid and ethanol by FTIR spectra, are shown in Fig 5. As can be seen, they are very similar in both processes that use DS methods and without DS. The spectral features can be related to those of ethyl oleate. Overall, the peak strong intensity of ethyl oleate uses DS methods more sharply than without DS. Comparization of functional groups between ethyl oleate standard with ethyl oleate experiment is shown in Table 3. The intensity of the peaks from the low to the high wave number, the major bands are associated with the attending vibrations [19]; [20]. The FTIR Spectra of ethyl oleate showed stretching vibration of the C-H, the shift at 2853-2854 cm^{-1} was due to anti-symmetrical stretching vibration of aliphatic C-H, and the band at 2922-2923 cm^{-1} was due to symmetrical stretching vibration of aliphatic C-H in CH_2 and terminal CH_3 groups, respectively [20]. The peak identified at 1735-1738 cm^{-1} proved the presence of H-C=O in-plane bending vibration, and the band at 1461-1462 cm^{-1} was $-\text{CH}_3$ asymmetric deformation vibration, respectively [21]. Band at 1372 cm^{-1} was due to H-C-H symmetric bending vibration and C-C stretching vibration at 1300-1301 cm^{-1} . The C-O-C asymmetrical stretching vibration at 1177-1178 cm^{-1} .

Meanwhile, the band is at 1033 cm^{-1} , which is ascribed to the C-O-C symmetric stretching vibration, which is a special characteristic in ethyl ester [20]. The wave number below 1000 cm^{-1} , band at 722-723 cm^{-1} , is for the overlapping of the $(\text{CH}_2)_n$ rocking vibration [21]. Further, no obvious -OH bond is detected, indicating no longer H_2O of ethyl oleate. Finally,

from FTIR analysis, it is clearly seen that ethyl oleate was successfully synthesized from oleic acid and ethanol.

3.3 Optimizing esterification with RSM modelling

RSM and Box-Behnken modeled the optimization of OA conversion. As shown in Table 5 with RSM and BBD experimental design as well as, the experimental and predicted OA conversion values, a total of 27 groups of experiments were carried out. According to the data in Table 5 and Table 6, and based on the fit summary from RSM modeling, a quadratic polynomial equation is suggested. Considering the obtained results, the final equation relating the esterification reaction with the most significant parameters evaluated is presented between the OA conversion and the various factors that best described the process as a function of actual values of the temperature reaction (X_1), concentration of catalyst (X_2), molar ratio of ethanol/OA (X_3), and reaction time (X_4) for OA conversion is given by Equation (3).

$$Y = 81.69 + 5.73 X_1 - 2.24 X_2 - 0.7173 X_3 - 0.8442 X_4 + 1.64 X_1 X_2 + 6.65 X_1 X_3 + 7.86 X_1 X_4 - 4.51 X_2 X_3 - 2.45 X_2 X_4 - 2.99 X_3 X_4 - 0.6001 X_1^2 + 8.24 X_2^2 - 1.49 X_3^2 - 2.94 X_4^2 \quad (3)$$

Where Y represents the conversion of OA, X_1 , X_2 , X_3 , and X_4 represent the reaction temperature, catalyst concentration, ethanol/OA molar ratio, and reaction time, respectively. It can be seen that X_1 , X_1X_2 , X_1X_3 , X_1X_4 , X_2^2 have a positive effect on the response. It means that the temperature reaction, the combination of the temperature reaction and catalyst concentration, the combination of temperature reaction and the ethanol/OA molar ratio, the combination of temperature reaction and reaction time, and the catalyst concentration² were influenced by OA conversion.

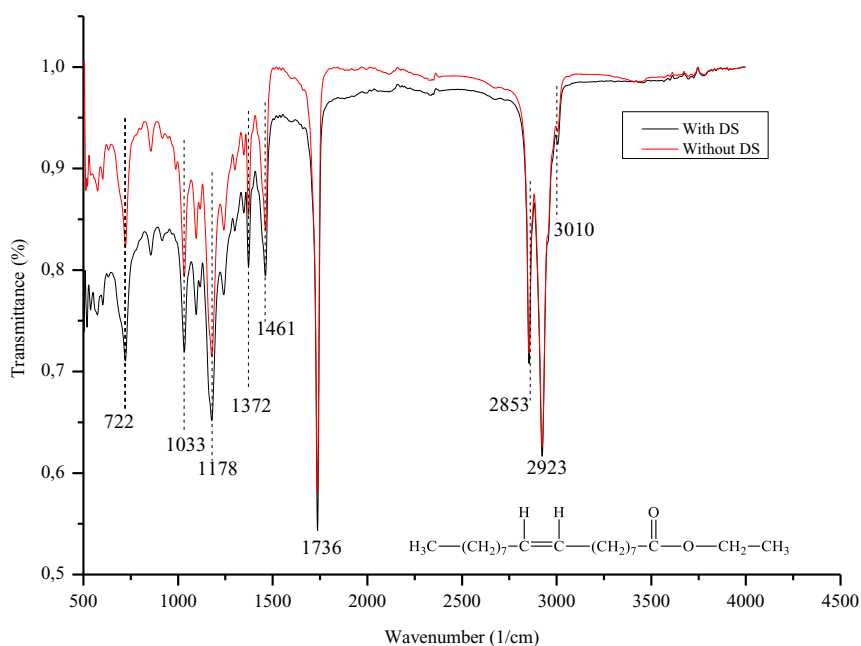


Fig. 5. FTIR spectra of esterification reaction between oleic acid and ethanol: with DS method (black line), without DS method (red line)

Table 3. Functional groups of ethyl oleate by FTIR

Functional groups	Wavenumber (cm ⁻¹)		
	Ethyl oleate standard [22]	Ethyl oleate with DS	Ethyl oleate without DS
Overlapping of the (CH ₂) _n	723	722	723
C-O-C symmetric stretching vibration	1056	1033	1033
C-O-C asymmetric stretching vibration	1244	1178	1177
C-C stretching vibration	1302	1300	1301
H-C-H symmetric bending vibration	1373	1372	1372
-CH ₃ asymmetric deformation vibration	1466	1462	1461
H-C=O- in-plane bending vibration	1739	1735	1738
-CH- anti-symmetric stretching vibration	2866	2853	2854
-CH- symmetric stretching vibration	2925	2923	2922
C-H stretching vibration	3003	3010	3008

The P value of the model was significant at X_1 , X_1X_4 , and X_2^2 , and the F-value of the model was significant at X_3 X_1^2 , as seen from Table 5, which indicates that the model is significant for the experimental results. A negative predicted R^2 implies that the overall mean may be a better predictor of OA conversion than the current model. In some cases, a higher-order model may also predict better. Adeq precision was 4.5189, indicating an adequate signal. The regression coefficient R^2 was 0.6410. It means that 64.10 % of the variables, namely temperature, catalyst concentration, ethanol/OA molar ratio, and reaction time, affect the OA conversion. There was a 23.29 % chance that an F-value this large could occur due to noise. This model temperature (X_1) and catalyst concentration (X_2^2) variables were a significant model term. The Lack of Fit F-value of 2.11 implies the Lack of Fit was not significant relative to the pure error. There was a 36.46 % chance that a Lack of Fit F-value this large could occur due to noise. A non-significant lack of fit was good for this model. Based on numerical variables, existing models are sufficient to predict OA conversion in the range of variables studied. The ethanol/OA molar ratio and reaction time of the impacting factor, P value in the model, was >0.1000 , indicating that these factors have no significant influence on the OA conversion. Therefore, the ethanol/OA molar ratio and reaction time affect the temperature reaction to a greater extent but have little effect on the overall reaction process.

3.4 3-D surface plot

The effect of the interaction of catalyst concentration and ethanol/OA molar ratio on OA conversion can be seen in Fig. 6. The response of the surface design is OA conversion using second-order non-linear models are Box-Behnken Design (BBD) in a 3D plot curve. The curve in Fig. 6 indicates the OA conversion gradually reached a peak with the ethanol/OA molar ratio and catalyst concentration increasing to a certain value. When the ethanol/OA

molar ratio and catalyst concentration continue to increase, the OA conversion decreases. It can be seen that run#24, with the catalyst concentration of 2 % and the ethanol/OA molar ratio of 10:1, produces the minimum OA conversion of 81.87 %.

Meanwhile, in run#10, the ethanol/OA molar ratio was 9:1, and the catalyst concentration was 3 %, giving the maximum OA conversion of 98.78 %. Obviously, increasing the ethanol/OA molar ratio has a positive impact on the reaction rate. Meanwhile, ethanol is found more in the molar ratio, which will reduce the OA concentration and the contact area between OA and catalyst, and excess ethanol can drive the reversible reaction in the positive direction during the esterification reaction [23]. The presence of the effect of the temperature and catalyst concentration on OA conversion is shown in Fig. 7. The temperature reaction is a more important factor affecting the reaction in experiments carried out at 80 °C, 90 °C, and 100 °C, as well as the catalyst concentration was carried out of 1 %, 2 %, and 3 % to explore the effect of temperature and catalyst concentration on OA conversion.

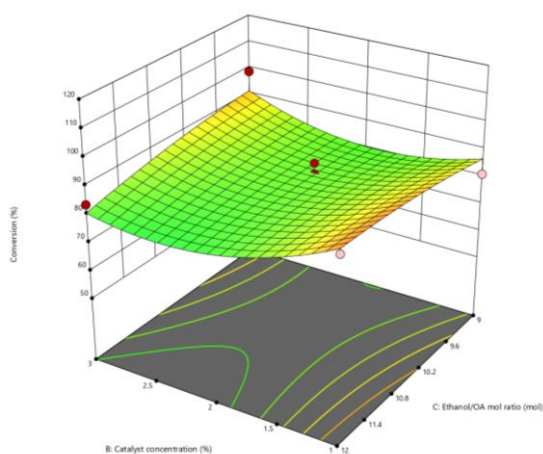


Fig. 6. Response surface plots of OA conversion versus catalyst concentration and ethanol/OA molar ratio

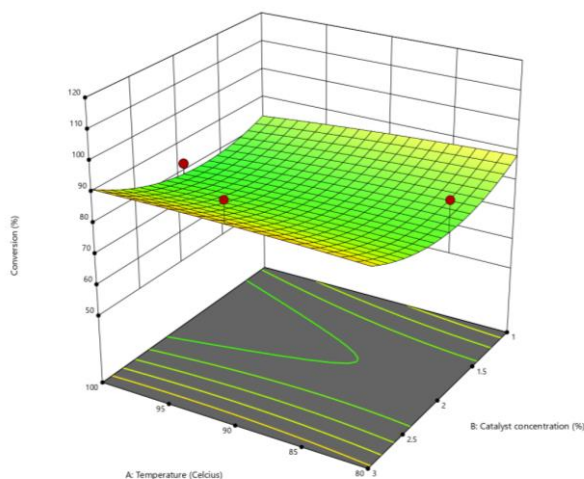


Fig. 7. Response surface plots of OA conversion versus temperature and catalyst concentration

As shown in Fig. 7, as the catalyst concentration increases from 1 % to 3 %, the OA conversion goes up from 81.23 % to 98.78 %, with temperature from 90 °C to 100 °C, which is mainly because increasing the catalyst concentration would cause the total amount of catalyst to rise. When the catalyst concentration increases, it causes the contact area between the reactants and the catalyst to become larger [24]. This can be interpreted as the continuous increase of the temperature, an increase in the catalyst activity, and its catalytic efficiency continues to improve. Additionally, the increasing temperature accelerates the collision between molecules, which has a positive impact on the esterification of ethanol and OA [25]; [26].

Fig. 8 shows the combined effect of the temperature and the ethanol/OA molar ratio on the OA conversion. It could be seen that run#26, when the ethanol/OA molar ratio was 12 :1 ; and temperature was 80 °C, gives the OA conversion of 58,54 % as well as run#18, when the ethanol/OA molar ratio was 10 :1. The temperature was 90 °C, resulting in the OA conversion of 85.87 %. It can be interpreted that a high ethanol/OA molar ratio is conducive to driving OA conversion. However, a lower molar ratio is useful for the positive esterification direction. As the temperature can be seen from the contour lines, high temperature or low temperature has an overall influence on the conversion. The extent of OA is clear.

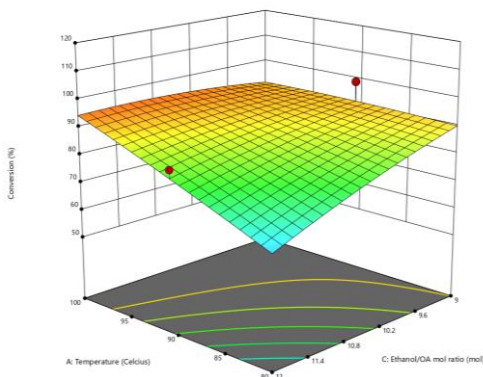


Fig. 8. Response surface plots of OA conversion versus temperature and ethanol/OA molar ratio

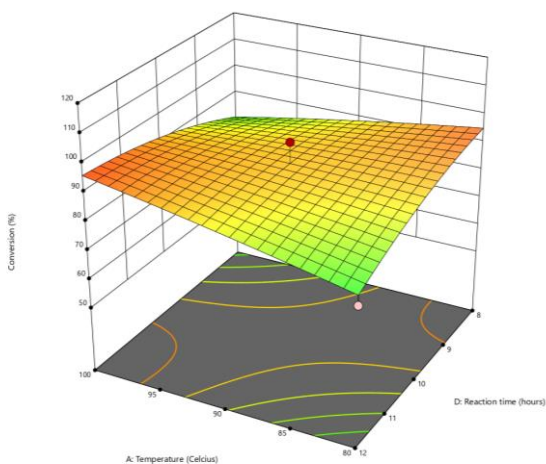


Fig. 9. Response surface plots of OA conversion versus temperature and reaction time

Fig. 9 identifies the influences of the temperature and reaction time on OA conversion in the esterification reaction. Fig. 9. It is not difficult to see from the 3D surface diagram that changes in temperature have a bigger impact on the OA conversion. In certain cases, the temperature range, the movement between reactant molecules, and their effective collision during the esterification process will increase in temperature [24]; [23]. It also has a positive effect on the removal of water molecules through the Dean-Strak method. It can be seen from the contour lines in the figure, that the reaction time has no obvious influence on OA conversion. The effects of both catalyst concentration and reaction time on the OA conversion are shown in Fig. 10. This proves that increasing the catalyst concentration can increase the OA conversion.

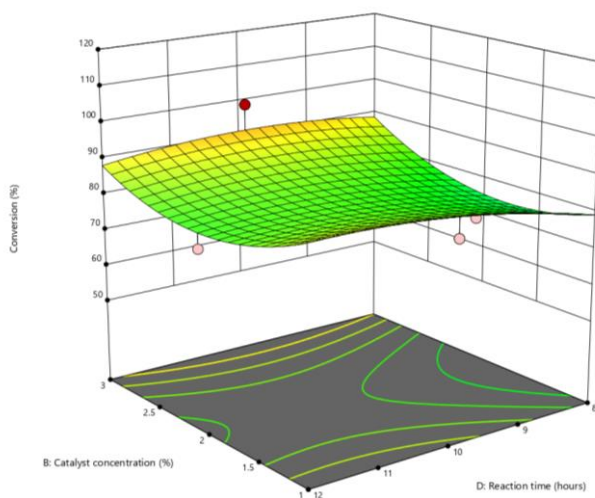


Fig. 10. Response surface plots of OA conversion versus catalyst concentration and reaction time

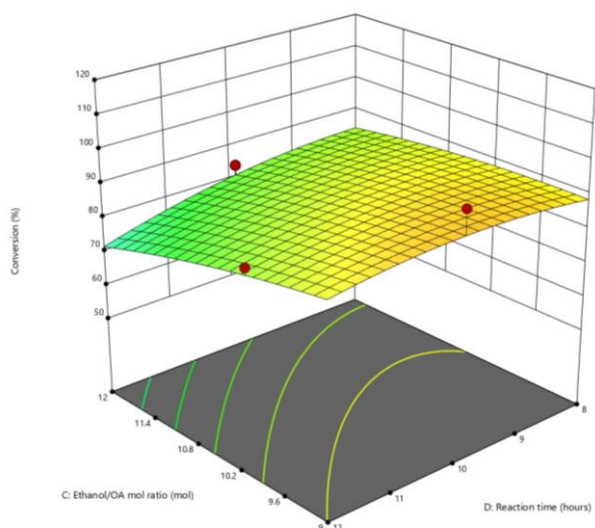


Fig. 11. Response surface plots of OA conversion versus ethanol/OA molar ratio and reaction time

However, based on contour lines, it can be seen the OA conversion did not change significantly when the reaction time level changed from low to high, which also verifies the reaction time does not affect the progress of the degree of the esterification reaction.

The combination effect of the ethanol/OA molar ratio and reaction time on the OA conversion is shown in Fig. 11. It can be seen from the contour lines that the high ethanol/OA molar ratio opportunity to promote the OA conversion, when run#3 with the ethanol/OA ratio was 12 :1, the reaction time was 12 hours can produce the OA conversion of 80.96 %. Also, when run#18 with the ethanol/OA molar ratio was 10 :1, the reaction time was 10 hours, resulting in the OA conversion of 85.87 %. In comparison, a higher reaction time is not advantageous for the positive direction of the esterification reaction. As for the ethanol/OA molar ratio, whether the low molar ratio or the high molar ratio has an overall effect on the OA conversion is not chiefly obvious.

Table 4. Experimental results and prediction of esterification response value

Run	Temperature reaction (°C)	Catalyst concentration (%)	Ethanol/OA molar ratio	Reaction time (hours)	Experimental OA conversion (%)	Predicted OA conversion (%)
1	80	3	9	12	75.56	79.01
2	90	1	10	12	90.54	90.40
3	90	2	12	8	88.54	80.38
4	80	1	10	10	93.87	88.28
5	100	2	10	8	80.31	73.72
6	90	1	9	10	81.23	86.89
7	80	2	9	10	91.56	81.24
8	100	2	10	12	90.49	89.75
9	80	2	12	10	58.54	66.50
10	90	3	9	10	98.78	91.43
11	80	2	10	8	81.36	82.42
12	100	1	10	10	95.86	92.00
13	90	2	9	12	75.87	80.13
14	90	3	10	12	86.06	84.04
15	90	2	12	12	80.96	72.71
16	90	3	10	8	84.94	88.63
17	100	3	10	10	88.65	93.83
18	90	2	10	10	85.87	81.76
19	90	1	10	8	83.09	85.20
20	90	2	10	10	74.09	81.76
21	90	2	10	10	81.87	81.76
22	80	2	10	12	63.56	67.01
23	90	2	9	8	67.94	75.83
24	90	3	12	10	83.94	80.98
25	90	1	12	10	92.65	94.47
26	100	2	12	10	81.67	91.27
27	100	2	9	10	82.98	79.39

Table 5. Analysis of variance for OA esterification

Source	Sum of squares	Degree of freedom	Mean square	F value	p-value
Model	1477.93	14	105.57	1.53	0.2329
X ₁ -Temperature	316.26	1	316.26	4.59	0.0535
X ₂ -Catalyst concentration	48.16	1	48.16	0.6983	0.4197
X ₃ -Ethanol/OA molar ratio	6.32	1	6.32	0.0916	0.7674
X ₄ -Reaction time	7.55	1	7.55	0.1095	0.7464
X ₁ X ₂	8.73	1	8.73	0.1266	0.7281
X ₁ X ₃	199.53	1	199.53	2.89	0.1147
X ₁ X ₄	264.81	1	264.81	3.84	0.0737
X ₂ X ₃	91.55	1	91.55	1.33	0.2717
X ₂ X ₄	25.65	1	25.65	0.3719	0.5534
X ₃ X ₄	39.96	1	39.96	0.5794	0.4612
X ₁ ²	2.03	1	2.03	0.0295	0.8666
X ₂ ²	383.62	1	383.62	5.56	0.0362
X ₃ ²	9.12	1	9.12	0.1322	0.7225
X ₄ ²	46.55	1	46.55	0.6749	0.4274
Residual	827.68	12	68.97		
Lack of Fit	755.92	10	75.59	2.11	0.3646
Pure Error	71.77	2	35.88		
Cor Total	2305.61	26			

Note: R² = 0.6410, Adj R² = 0,2222, Pred R² = -1.3235, Adeq precision = 4.5189

Table 6. Coefficient post analysis with RSM and BBD Design

	Intercept	X ₁	X ₂	X ₃	X ₄	X ₁ X ₂	X ₁ X ₃	X ₁ X ₄
Conversion	81.69	5.73	-2.24	-0.7173	-0.8442	1.64	6.65	7.86
p-values		0.05	0.41	0.76	0.74	0.72	0.11	0.07

Table 7. Coefficient post analysis with RSM and BBD Design (continued)

	X_2X_3	X_2X_4	X_3X_4	X_1^2	X_2^2	X_3^2	X_4^2
Conversion	-4.51	-2.45	-2.99	-0.6001	8.24	-1.49	-2.94
p-values	0.27	0.55	0.46	0.86	0.03	0.72	0.42

3.5 Optimizing of OA conversion

According to the predicted results of RSM analysis when the temperature reaction was 98.55 °C, the catalyst concentration was 1.13 %, the ethanol/OA molar ratio was 11.69, and the reaction time was 10.49 hours, the predicted optimal OA conversion was 100.45 %. The experiments were carried out at optimal reaction conditions to verify the accuracy of the model. The results show that the OA conversion was 99.87 ± 0.6 %, which illustrates that the model prediction was reliable.

The experimental and the predicated RSM models of the OA conversion, and the model's residuals are presented in Fig. 12. The residual values were obtained by calculating the difference between the experimental and the RSM model values. In conclusion, optimization studies of ethyl oleate from ethanol and oleic acid with Dean-stark trap technology by RSM were successful.

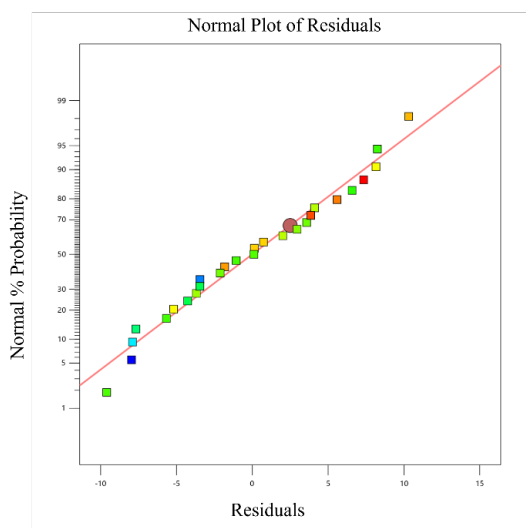


Fig. 12. Response surface plots of OA conversion between normal and residuals

4 Conclusion

Referring to this research, the esterification reaction using a Dean-stark trap and without a Dean-stark trap method between ethanol and OA was studied, and characterization of the molecular structure with FTIR and GC-MS of esterification with these methods was established as well. The influence of the temperature reaction, the catalyst concentration, the ethanol/OA molar ratio, and the reaction time on the esterification reaction were all investigated. The obtained OA conversion was 98.78 % when the optimal conditions for the esterification reaction using a Dean-stark method with 90 °C temperature reaction, 3 %

catalyst, 9:1 molar ratio ethanol/OA, and 10 hours reaction time. Based on that data, the response surface methods (RSM) were used to fit and optimize the experimental data. They showed the optimization of the esterification process satisfactory alignment scheme results with the experimental results. Therefore, the esterification reaction using the DS method promotes the esterification use with different types of alcohol sources.

This research was supported by the Research Center for Chemistry, National Research and Innovation Agency (BRIN), Degree by Research Program from BRIN, and Department of Chemical Engineering, Faculty of Engineering, Universitas Indonesia. The author also expresses gratitude to ELSA-BRIN for characterization and data analysis in this work.

References

- [1] R. C. Larock and R. Rozhkov, *Inverconversion of Nitriles, Carboxylic Acids, and Derivatives*, vol. 3049, no. 2010. 2018. doi: 10.1002/9781118662083.cot09-009.
- [2] K. Monroe, T. Kirk, V. Hull, E. Biswas, A. Murawski, and R. L. Quirino, *Vegetable Oil-Based Polymeric Materials: Synthesis, Properties, and Applications*, no. c. Elsevier Ltd., 2020. doi: 10.1016/b978-0-12-803581-8.11521-8.
- [3] A. G. A. SÁ, A. C. de Meneses, P. H. H. de Araújo, and D. de Oliveira, 'A review on enzymatic synthesis of aromatic esters used as flavor ingredients for food, cosmetics and pharmaceuticals industries', *Trends in Food Science and Technology*, vol. 69, pp. 95–105, 2017, doi: 10.1016/j.tifs.2017.09.004.
- [4] J. H. Steele, M. X. Bozor, and G. R. Boyce, 'Transmutation of Scent: An Evaluation of the Synthesis of Methyl Cinnamate, a Commercial Fragrance, via a Fischer Esterification for the Second-Year Organic Laboratory', *Journal of Chemical Education*, vol. 97, no. 11, pp. 4127–4132, 2020, doi: 10.1021/acs.jchemed.0c00861.
- [5] Z. Khan et al., 'Current developments in esterification reaction: A review on process and parameters', *Journal of Industrial and Engineering Chemistry*, vol. 103, pp. 80–101, 2021, doi: 10.1016/j.jiec.2021.07.018.
- [6] Z. Khan et al., 'Current developments in esterification reaction: A review on process and parameters', *Journal of Industrial and Engineering Chemistry*, vol. 103, pp. 80–101, 2021, doi: 10.1016/j.jiec.2021.07.018.
- [7] B. Ali, N. A. Al-wabel, S. Shams, A. Ahamad, S. A. Khan, and F. Anwar, 'Essential Oils Used in Aromatherapy: A Systemic Review', *Asian Pacific Journal of Tropical Biomedicine*, vol. 5, no. 8, pp. 601–611, 2015, doi: 10.1016/j.apjtb.2015.05.007.
- [8] G. Jyoti, A. Keshav, and J. Anandkumar, 'Experimental and Kinetic Study of Esterification of Acrylic Acid with Ethanol Using Homogeneous Catalyst', *International Journal of Chemical Reactor Engineering*, vol. 14, no. 2, pp. 571–578, 2016, doi: 10.1515/ijcre-2015-0131.
- [9] S. Bertouche, V. Tomao, K. Ruiz, A. Hellal, C. Boutekedjiret, and F. Chemat, 'First approach on moisture determination in food products using alpha-pinene as an alternative solvent for Dean-Stark distillation', *Food Chemistry*, vol. 134, no. 1, pp. 602–605, 2012, doi: 10.1016/j.foodchem.2012.02.158.
- [10] L. A. Sarabia and M. C. Ortiz, '12 Response Surface Methodology', in *Comprehensive Chemometrics - Chemical and Biochemical Data Analysis*, R. T. and B. W. Steven D. Brown, Ed., Elsevier B.V., 2009, pp. 345–390, Volume 1.
- [11] D. C. Montgomery, *Design and Analysis of Experiments*, 9th ed. Arizona: John Wiley & Sons, Inc., 2017.
- [12] C. G. Mbah, C. V. Esonye, D. O. Onukwuli, and V. Chukwuemeka, 'USE OF RESPONSE SURFACE METHODOLOGY (RSM) IN OPTIMISATION OF BIODIESEL PRODUCTION FROM COW TALLOW', 2021.

- [13] F. Naidir, R. Yunus, I. Ramli, and T. I. Mohd Ghazi, 'Response surface methodology for optimization of epoxidized trimethylolpropane ester synthesis from palm oil', *International Journal of Chemical Reactor Engineering*, vol. 9, 2011, doi: 10.1515/1542-6580.2677.
- [14] J. Manga, A. Ahmad, P. Taba, and Firdaus, 'Optimization synthesis fatty acid ethyl ester as biodiesel from palm fatty acid distillate using $\text{SO}_4^{2-}/\text{TIO}_2$ catalyst supported by mesoporous silica', *Rasayan Journal of Chemistry*, vol. 13, no. 1, pp. 621–627, 2020, doi: 10.31788/RJC.2020.1315494.
- [15] 'NIST/EPA/NIH Mass Spectral Library Compound Scoring: Match Factor, Reverse Match Factor, and Probability'.
- [16] N. I. Madondo and M. Chetty, 'Anaerobic co-digestion of sewage sludge and bio-based glycerol: Optimisation of process variables using one-factor-at-a-time (OFAT) and Box-Behnken Design (BBD) techniques', *South African Journal of Chemical Engineering*, vol. 40, pp. 87–99, Apr. 2022, doi: 10.1016/j.sajce.2022.02.003.
- [17] I. Veza, M. Spraggon, I. M. R. Fattah, and M. Idris, 'Response surface methodology (RSM) for optimizing engine performance and emissions fueled with biofuel: Review of RSM for sustainability energy transition', *Results in Engineering*, vol. 18. Elsevier B.V., Jun. 01, 2023. doi: 10.1016/j.rineng.2023.101213.
- [18] B. Ricetti Margarida, L. I. Flores, L. F. De Lima Luz Jr., and M. Kaminski Lenzi, 'Optimization of Esterification Reaction Conditions Through the Analysis of the Main Significant Variables', *Angolan Industry and Chemical Engineering Journal*, vol. 1, no. 1, pp. 6–11, 2021, doi: 10.47444/aincej.v1i1.6.
- [19] P. de la Mata, A. Dominguez-Vidal, J. M. Bosque-Sendra, A. Ruiz-Medina, L. Cuadros-Rodríguez, and M. J. Ayora-Cañada, 'Olive oil assessment in edible oil blends by means of ATR-FTIR and chemometrics', *Food Control*, vol. 23, no. 2, pp. 449–455, Feb. 2012, doi: 10.1016/j.foodcont.2011.08.013.
- [20] S. Niu, Y. Zhou, H. Yu, C. Lu, and K. Han, 'Investigation on thermal degradation properties of oleic acid and its methyl and ethyl esters through TG-FTIR', *Energy Conversion and Management*, vol. 149, pp. 495–504, 2017, doi: 10.1016/j.enconman.2017.07.053.
- [21] H. Li, S. L. Niu, C. M. Lu, and S. Q. Cheng, 'Comparative evaluation of thermal degradation for biodiesels derived from various feedstocks through transesterification', *Energy Conversion and Management*, vol. 98, pp. 81–88, Jul. 2015, doi: 10.1016/j.enconman.2015.03.097.
- [22] Chemical Book, 'Ethyl oleate_Reff', ChemicalBook All rights reserved. Accessed: Oct. 05, 2023. [Online]. Available: https://www.chemicalbook.com/SpectrumEN_111-62-6_IR1.htm
- [23] W. Jiang, J. Zhu, Z. Yuan, J. Lu, and J. Ding, 'Optimization of the esterification of oleic acid and ethanol in a fixed bed membrane reactor by response surface method', *Fuel*, vol. 342, no. February, p. 127867, 2023, doi: 10.1016/j.fuel.2023.127867.
- [24] Andy Wells, 'Introduction to General, Organic and Biochemistry', 2023.
- [25] H. Gan, S. A. Hutchinson, C. Hurren, Q. Liu, X. Wang, and R. L. Long, 'Effect of oleic purity on the chemical structure, thermal and rheological properties of bio-based polymers derived from high oleic cottonseed oil via RAFT polymerization', *Industrial Crops and Products*, vol. 171, no. October 2020, p. 113882, 2021, doi: 10.1016/j.indcrop.2021.113882.
- [26] N. Allif Fathurrahman, M. Nasikin, Y. Yulizar, and M. Khalil, 'Thermodynamic study on the prevention of B30 biodiesel wax crystallization by $\gamma\text{-Al}_2\text{O}_3$ nanoparticles and sorbitan monooleate', *Fuel*, vol. 314, no. December 2021, p. 123144, 2022, doi: 10.1016/j.fuel.2022.123144.